Protein structure in model infant milk formulas impacts their kinetics of hydrolysis under in vitro dynamic digestion

Amira Halabi, Thomas Croguennec, Olivia Ménard, Valérie Briard-Bion, Julien Jardin, Yann Le Gouar, Marie Hennetier, Said Bouhallab, Didier Dupont, Amélie Deglaire

Food Hydrocolloids 126 (2022) 107368

Contents lists available at ScienceDirect

Food Hydrocolloids

journal homepage: www.elsevier.com/locate/foodhyd

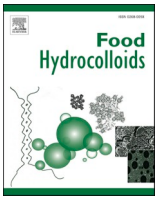

Protein structure in model infant milk formulas impacts their kinetics of hydrolysis under *in vitro* dynamic digestion

Amira Halabi [a], Thomas Croguennec [a], Olivia Ménard [a], Valérie Briard-Bion [a], Julien Jardin [a], Yann Le Gouar [a], Marie Hennetier [b], Saïd Bouhallab [a], Didier Dupont [a], Amélie Deglaire [a,*]

[a] *STLO, INRAE, Institut Agro, 35042, Rennes, France*
[b] *Université de Toulouse, Institut National Polytechnique de Toulouse – Ecole d'Ingénieurs de Purpan, Département Sciences Agronomiques et Agroalimentaires, 31076, Toulouse Cedex 03, France*

ARTICLE INFO

Keywords:
Infant formula
Heat treatment
Milk protein structure
Dynamic *in vitro* digestion

ABSTRACT

The impact of protein structure in model infant milk formulas (IMFs) on digestion was evaluated using an *in vitro* dynamic digestion model. IMFs differed by their whey protein profile and the heating conditions. Digesta microstructure was followed by laser light scattering and confocal laser scanning microscopy. Proteolysis kinetics were monitored by SDS-PAGE and OPA assay and peptide release kinetics by tandem mass spectrometry. The gastric digesta microstructure depended on the protein structure within IMFs, with the highest protein particle size in IMF containing native casein micelles. Among whey proteins, denatured/aggregated lactoferrin was the most sensitive to pepsin hydrolysis. The peptidomic profile during digestion varied among IMFs. More numerous and resistant intestinal bioactive peptides were observed for the unheated IMF having a whey protein profile closer to that of human milk. Further physiological studies are required to investigate the benefits of adapting the IMF whey protein profile on infant health.

1. Introduction

When breastfeeding is not possible or cannot be considered, infant milk formulas (IMFs) constitute the sole adequate human milk substitute. The challenge for IMF manufacturers is to mimic as much as possible the gross composition of human milk. Currently, IMFs are formulated mostly based on bovine milk, presenting a different whey protein profile to that of human milk. Dietary proteins provide nitrogen and indispensable amino acids required not only for body protein synthesis but also for other nitrogenous compounds implied in diverse functions such as neurodevelopment or hormonal regulation (Michaelsen & Greer, 2014). In addition, dietary proteins, particularly those present in human milk (e.g. lactoferrin or α-lactalbumin) exert some bioactive properties (immunomodulatory, antibacterial, etc) either directly or after bioactive peptide release (Layman et al., 2018; Lönnerdal, 2016; Wang et al., 2019). Better simulating the protein profile of human milk in IMFs could lead to better health outcomes for the infants. This may be achieved through the supplementation of IMFs with purified bovine milk proteins such as α-lactalbumin and lactoferrin, the major whey proteins in human milk. Due to the high proportion of essential amino acids in α-lactalbumin, the α-lactalbumin supplementation allows the reduction of the IMF protein content while respecting the regulatory aminogram and supporting age growing (Davis et al., 2008; Trabulsi et al., 2011). This is of particular importance since a high protein content in IMFs has been attributed to the obesity onset in children (Totzauer et al., 2018). In addition, the amino acid bioavailability may be improved, particularly for tryptophan, a precursor of serotonin and melatonin (Sandström et al., 2008). The lactoferrin supplementation can present some health benefits such as antibacterial and immunomodulatory activities and an enhanced iron bioavailability (Lönnerdal, 2009).

IMF manufacturing consists of a succession of steps during which heat treatments are applied to guarantee the microbiological safety and to extend the shelf life. Depending on the heating conditions, the extent of whey protein denaturation and the structure of milk proteins are differently affected (Halabi, Deglaire, Hamon, et al., 2020; Halabi, Deglaire, Hennetier, et al., 2020), impacting the functional properties and nutritional value of IMFs. We have previously shown that the rapid destabilization of the native casein micelles under gastric conditions resulted in the formation of large aggregates that slowed down the

* Corresponding author.
E-mail address: amelie.deglaire@agrocampus-ouest.fr (A. Deglaire).

https://doi.org/10.1016/j.foodhyd.2021.107368
Received 6 September 2021; Received in revised form 25 October 2021; Accepted 13 November 2021
Available online 20 December 2021

casein pepsinolysis, and that the gastric hydrolysis of denatured lactoferrin was drastically enhanced at the very beginning of the digestion (Halabi, Croguennec, et al., 2020). Nevertheless, this was observed using a static *in vitro* digestion model which, despite its usefulness for a first screening, does not simulate the dynamic and more physiological parameters such as the continuous pH monitoring, digestive fluid secretion and gastric and intestinal emptying. Therefore, dynamic *in vitro* digestion models have been developed to better mimic the *in vivo* digestion process, particularly the kinetics of protein hydrolysis, such as reported by Egger et al. (2019). These kinetics have physiological consequences, as it impacts the kinetics of amino acid absorption and thus the nitrogen metabolic fate.

In the present paper, the influence of protein composition and structure within IMFs on digestion kinetics was investigated using a dynamic *in vitro* model at the term newborn stage. The DIDGI® *in vitro* dynamic simulator used in the present study has been previously validated towards *in vivo* data for its relevance to simulate infant formula digestion (Ménard et al., 2014). Two model IMFs were formulated with the same protein content (1.3% proteins; casein:whey protein ratio of 40:60) but with a different whey protein profile. The Control IMF had a whey protein profile close to that of commercial IMFs. The LF^+ α-LA^+ IMF had a whey protein profile close to that of human milk. The IMFs were unheated or heated at 80 °C to reach 65–70% of denatured whey proteins, value within the range found in commercial IMFs. During digestion, the IMF destabilization was studied by laser light scattering and confocal laser scanning microscopy (CLSM), the kinetics of protein hydrolysis was investigated both by SDS-PAGE under reducing conditions and OPA (*o*-phthalaldehyde) assay. The kinetics of peptide release was followed by tandem mass spectrometry, and protein digestibility was estimated at the final digestion point by nitrogen measurement after a 10-kDa ultrafiltration.

2. Material and methods

2.1. Materials

2.1.1. Infant milk formula ingredients

Low-heat skimmed milk powder (SMP) was obtained by microfiltration, concentration and spray-drying of raw skimmed milk (Fromagerie Gillot, Saint-Hilaire-de-Briouze, France) at the semi-industrial unit Bionov (Rennes, France). SMP was characterized by a whey protein nitrogen index of 9 mg of nitrogen per g of powder and a protein content of 36%, as determined by Kjeldhal method (N x 6.38). Whey protein isolate (WPI; Prolacta®95) was purchased from Lactalis Ingredients (Bourgbarré, France). Bovine lactoferrin powder (Prodiet Lactoferrin®) and bovine α-lactalbumin powder were kindly provided by Ingredia Dairy Experts (Arras, France) and Agropur Inc (Appleton, USA), respectively. The protein content of the WPI, lactoferrin and α-lactalbumin powders was 88, 90 and 84% (w/w), respectively, as determined by Kjeldhal method (N x 6.38). All protein powders were stored at −20 °C until use. Lactose was supplied by Armor Proteines (Saint- Brice-en-Coglès, France). $CaCl_2{\cdot}2H_2O$ was from AnalaR (Leuven, Belgium), $FeSO_4{\cdot}7H_2O$ from Sigma- Aldrich (St-Louis, USA), KCl from Panreac (Barcelona, Spain), $Na_3PO_4{\cdot}12H_2O$ from Merck (Darmstadt, Germany), and $Na_3C_6H_5O_7{\cdot}2H_2O$ from Carlo Erba Reagents (Val-de-Reuil, France). Water was Milli-Q water.

2.1.2. In vitro digestion material

Pepsin was from porcine gastric mucosa (P6887; 3075 U/mg). Pancreatin was from porcine pancreas (P7545; trypsin activity of 6.7 U/mg; lipase activity of 85.2 U/mg). Bile extract was from bovine bile (B3883; 0.9 mmol/g). The enzyme activities and bile concentration were measured using the assays described by Brodkorb et al. (2019). Enzymes and bile salts, as well as protease inhibitors namely Pepstatin A (P5318), Pefabloc® SC (76307) and Pefabloc® SC PLUS (11873601001), were purchased from Sigma-Aldrich (St. Quentin Fallavier, France).

2.2. Preparation of the infant milk formulas

The IMFs were produced as described previously (Halabi, Croguennec et al., 2020), with a final composition of 1.32 ± 0.02 g of proteins (casein:whey protein ratio of 40:60) and 5.63 ± 0.01 g of lactose per 100 g of liquid IMFs. The IMFs only differed by their whey protein profile, with 0.16 g ± 0.00 of α-lactalbumin and 0.54 g ± 0.01 of β-lactoglobulin per 100 g of liquid control IMF, or 0.47 g ± 0.00 of α-lactalbumin, 0.06 g of β-lactoglobulin and 0.19 g ± 0.01 of lactoferrin per 100 g of liquid LF^+α-LA^+ IMF, as determined by reverse-phase high performance liquid chromatography (RP-HPLC).

After an equilibration time at 30 °C for 60 min, glass tubes containing 10 mL of IMFs were pre-heated in a water bath to reach 53.5 °C, then placed in a water bath at 80 °C during 9 min or 30 min for the control or LF^+α-LA^+ IMFs, respectively, to reach the same protein denaturation rate in both IMFs. After heating, the IMF samples were cooled by immersion in an ice-water bath and pooled. Each heat treatment was repeated three times on three freshly prepared IMF (n = 3). The unheated IMFs were used as reference. The heat-induced denaturation extent of total whey proteins was 69% for the control IMF and 68% for the LF^+α-LA^+ IMF, as determined by RP-HPLC. Unheated and heated IMFs were stored at 4 °C before *in vitro* digestion experiment. The protein structures obtained by varying the whey protein profile of IMFs and the heating conditions, characterized by asymmetric flow field flow fractionation coupled with multiangle light scattering and differential refractometer (AF_4-MALS-dRi) (Halabi, Deglaire, Hennetier, et al., 2020), are described in the Supplementary Table 1.

2.3. In vitro digestion protocol

In vitro gastrointestinal digestion of the IMFs was carried out following a dynamic model using the bi-compartmental system DIDGI® (Ménard et al., 2015). The system was set up to simulate the gastrointestinal digestion conditions of term infants at the postnatal age of 4 weeks as described by de Oliveira et al. (2016) with some adaptation to the IMF-fed infants. The gastric emptying coefficients ($t_{1/2}$ = 78 min; β = 1.2) and the intestinal emptying coefficients ($t_{1/2}$ = 200 min; β = 2.2) were fixed according to Bourlieu et al. (2014). The gastric pH followed a linear regression pH = - 0.0155 x t + pH_{IMF} with t the digestion time (min) and pH_{IMF} the pH of undigested IMF (6.82 ± 0.03). The intestinal pH was maintained at 6.6. The variation of gastric pH was controlled using 0.5 M HCl and the intestinal pH was neutralized using 0.5 M $NaHCO_3$. Pepsin was diluted in simulated gastric fluid, composed of 94 mM NaCl and 13 mM HCl (pH 6.5), to 268 U/mL of total gastric volume. Pancreatin and bile were diluted in simulated intestinal fluid, composed of 164 mM NaCl, 10 mM KCl and 3 mM $CaCl_2$ (pH 6.6), to 7.1 U of trypsin/mL of total intestinal volume and 3.1 mmol/L of total intestinal volume, respectively.

Digestions were performed over 180 min. Samples were collected before digestion (undigested samples) and during both gastric and intestinal digestions at 40, 80, 120 and 180 min (G40, G80, G120, G180 for the gastric samples or I40, I80, I120, I180 for the intestinal samples). The emptied intestinal fraction was continuously collected on ice with regular addition of Pefabloc® as enzyme inhibitor. Except for laser light scattering and confocal microscopy analysis performed immediately after sampling, proteolysis was inhibited by adding 10 μL of Pepstatin A (0.73 mM in methanol) per mL of gastric digesta or 50 μL of Pefabloc® SC (0.1 M in distilled water) per mL of intestinal digesta. For mass spectrometry analysis, 50 μL of Pefabloc® SC PLUS (0.1 M in distilled water) per mL of intestinal digesta were added. Samples were stored at −20 °C until analysis. Each *in vitro* digestion experiment was performed in triplicate (n = 3).

2.4. Digesta microstructure characterization

2.4.1. Particle size distribution

Particle size distribution of the undigested IMFs and digesta was measured by laser light scattering using a Malvern Mastersizer 2000 (Malvern Instruments Ltd., Worcestershire, UK) as described previously (Halabi, Croguennec, et al., 2020). Particle size measurement was performed in triplicate for each sample and for each *in vitro* digestion experiments (n = 3).

2.4.2. Confocal laser scanning microscopy

The microstructure of the undigested IMFs and digesta was observed by confocal laser scanning microscopy (CLSM) using a ZEISS LSM880 inverted confocal microscope (Carl Zeiss AG, Oberkochen, Germany) at ×20 magnification. Samples (200 μL) were gently mixed with Fast Green aqueous solution (1% w/v; 6 μL) and the mixture was kept at room temperature for at least 10 min. 20 μL of mixture was deposited on a glass slide in a spacer and a cover slip was placed on top of all samples. Fast green was excited using a He–Ne laser system at a wavelength of 633 nm at a 1.72 μs pixel dwell scanning rate and detected using a PMT between 635 and 735 nm. Images were processed using confocal acquisition software ZenBlack and recorded in a panorama mode of 2 × 2 images at a resolution of 1944 × 1944 pixels each. Confocal analysis was performed for each *in vitro* digestion experiments (n = 3), with at least 10 micrographs recorded for each sample.

2.5. Proteolysis kinetics

2.5.1. SDS-PAGE and intact protein semi-quantification

The undigested IMFs and digesta were analyzed by SDS-PAGE under reducing conditions as previously described (Halabi, Croguennec, et al., 2020). The sample volume loaded on the gel slots was determined based on a loading equivalent to 5 or 30 μg of proteins from the undigested IMFs in the gastric or intestinal phase, respectively. The digesta volume loaded on the gel was then kept constant along the gastric or intestinal kinetics. The intact proteins remaining in the samples after dilution, emptying and hydrolysis were determined according to Equation (1).

$$\text{Intact protein } (\%) = \frac{\text{Protein peak area}_{\text{Digesta}}}{\text{Protein peak area}_{\text{Undigested IMF}}} \text{ x } 100 \quad (1)$$

2.5.2. OPA assay and degree of hydrolysis

The primary amino group quantification of undigested IMFs and digesta was performed using the OPA method as described previously (Halabi, Croguennec, et al., 2020). The degree of hydrolysis (DH) was calculated according to Equation (2), after considering the meal dilution and emptying by the gastrointestinal secretions.

$$\text{DH } (\%) = \frac{[NH_{2\text{digesta}}] - [NH_{2\text{secretions}}] - [NH_{2\text{undigested IMF}}]}{[NH_{2\text{total}}] - [NH_{2\text{undigested IMF}}]} \text{ x } 100 \quad (2)$$

with [$NH_{2\ \text{undigested IMF}}$] or [$NH_{2\ \text{digesta}}$] the primary amino group content in the undigested IMFs or in the digesta, respectively. [$NH_{2\ \text{secretions}}$] was the primary amino group content of bile and pancreatin solutions at the same concentrations as those found in intestinal digesta. [$NH_{2\ \text{total}}$] was the total content of primary amino groups within the IMFs after acid hydrolysis by 6 N HCl at 110 °C for 24 h. All the primary amino group contents were expressed in mg/L of IMF in order to consider the dilution factor during digestion.

2.6. In vitro protein digestibility

The digestible nitrogen content was determined by the micro-Kjeldahl method after centrifugation (9,000×*g*, 10 min, 4 °C) and 10 kDa-ultrafiltration (Vivaspin® 20, 10 000 K MWCO, PES, Sartorius Stedim Lab Ltd, Stonehouse, UK) operated at 9,000×*g* during 40 min at 4 °C. This was performed on the intestinal digesta at 180 min of digestion (I180) and on the intestinal fraction emptied over 180 min (I180E). *In vitro* protein digestibility was calculated for each type of digesta according to the two calculations presented below (Equations (3) and (4)) and was then averaged according to the meal repartition between the two types of digesta.

$$\text{Overall } \textit{in vitro} \text{ protein digestibility } (\%) = \frac{[\text{Digestible N}_{\text{digesta}}] - [\text{Digestible N}_{\text{secretions}}]}{[\text{Total N}_{\text{undigested IMF}}] \text{ x } \% \text{ substrate}} \text{ x } 100 \quad (3)$$

$$\text{Instantaneous } \textit{in vitro} \text{ protein digestibility } (\%) = \frac{[\text{Digestible N}_{\text{digesta}}] - [\text{Digestible N}_{\text{secretions}}]}{[\text{Total N}_{\text{digesta}}] - [\text{Total N}_{\text{secretions}}]} \text{ x } 100 \quad (4)$$

[Digestible $N_{digesta}$] was the N content (g of N/L of digesta) measured after centrifugation and 10 kDa-ultrafiltration of the I180 or I180E samples. [Total $N_{secretions}$] or [Digestible $N_{secretions}$] was the N content (g of N/L of digesta) in a solution containing bile and pancreatin at the same concentration than those found in the corresponding digesta or after its centrifugation and 10 kDa-ultrafiltration, respectively. [Total $N_{\text{undigested IMF}}$] was the total nitrogen content (g of N/L of IMF) in the IMF before digestion. % substrate was the estimated proportion of undigested IMF in the digesta (g/100 g of digesta) based on the emptying equations and on the secretion flows into the simulator. [Total N_{digesta}] was the N content (g of N/L of digesta) in the digesta.

2.7. Statistical analysis

All data are reported as means ± standard deviation (SD). Data statistical analysis was performed using the R software (version 3.6.1). Residual intact protein and DH variables were analyzed using a mixed linear model for repeated measures (nlme package). "Time", "Formula" (2 levels: control IMF – LF^{+} α-LA^{+} IMF) and "Treatment" nested within "Formula" (2 levels: unheated – heated at 80 °C) were considered as fixed factors, and digestion replicates were designated as random factor. Residual normality and variance homogeneity for each factor were tested for all variables with Shapiro-Wilk test and Levene test, respectively (lawstat package). When data were not conformed to the previous conditions, Box-Cox transformation was performed (MASS package). *In vitro* protein digestibility variable was analyzed using a linear model with "Formula" and "Treatment" nested within "Formula" as fixed factors. When differences were significant ($p < 0.05$), pairwise multiple comparison of the means was carried out using Tukey's test (lsmeans package).

2.8. Peptidomic analysis

2.8.1. Peptide identification and quantification

The undigested IMFs and digesta were analyzed by mass spectrometry as described previously (Deglaire et al., 2019) with some modifications. A nano-RSLC Dionex U3000 system fitted to a Q-Exactive mass spectrometer (Thermo Scientific, San Jose, USA) equipped with a nanoelectrospray ion source was used. After protein content adjustment in the acid buffer of the chromatographic system (200 ng of dietary proteins), 5 μL of samples were loaded onto a PepMap RSLC column (C18 column, 75 μm i.d. × 150 mm length, 3 μm particle size, 100 Å pore size; Dionex) equipped with a micro-precolumn pepMap100 (C18 column, 300 μm i.d. × 5 mm length, 5 μm particle size, 100 Å pore size; Dionex, Amsterdam, The Netherlands). Peptide separation was performed at a flow rate of 0.3 μL min^{-1} using solvent A [2% (v/v) acetonitrile, 0.08% (v/v) formic acid and 0.01% (v/v) TFA in HPLC gradient grade water] and solvent B [95% (v/v) acetonitrile, 0.08% (v/v) formic acid and 0.01% (v/v) TFA in HPLC gradient grade water]. The elution gradient first rose from 5 to 35% solvent B over 30 min, then up to 85% solvent B over 5 min before column reequilibration.

The mass spectra were recorded in positive mode using the m/z range 250–2000. The resolution of the mass analyzer was set in the acquisition method to 70 000 for MS and 17 500 for MS/MS. For each MS scan, the ten most intense ions were selected for MS/MS fragmentation and excluded from fragmentation for 10 s. Peptides were identified from the MS/MS spectra using the X!TandemPipeline C++ software (version 2017.2.1.4) against a database composed of reviewed proteins of "Bos Taurus" downloaded from Uniprot (https://uniprot.org; 6905 reviewed proteins) to which was added the common Repository of Adventitious Protein (http://thegpm.org/crap).

Database search parameters were specified as follows: nonspecific enzyme cleavage; a 0.05 Da mass error for fragment ions; 10 ppm mass error for parent ions The possible post-translational modifications were serine or threonine phosphorylation, methionine oxidation, lysine or arginine lactosylation, cyclisation of glutamine or glutamic acid into pyroglutamic acid and acetylation of cysteine, serine, lysine or any amino acid in N-ter position.

Peptides identified with an e-value < 0.01 were automatically validated. A minimum of 2 peptides was authorized to validate a protein. Peptides with a minimal length of 6 amino acids were considered. When a peptide was measured with several charge states, all ion intensities were summed. Peptide number represented the number of unique peptide sequences identified despite sequence modifications. Abundance corresponded to the area under the curve of the eluted peak (ion intensity).

2.8.2. Peptidomic data analysis

Peptide data analysis was performed using the R software (version 3.6.1). Peptides were considered for analysis if they were detected in at least 2 out of 3 digestion replicates. Visualization of the amounts of common or specific peptides among the IMFs was carried out using a Venn diagram (VennDiagram package).

The abundance of each peptide, determined at each digestion time, was log10-transformed [log10(abundance + 1)] and the maximum abundance was set to 1. Missing abundances were set at 0. Hierarchical clustering of the peptides identified in the undigested, gastric and intestinal samples (n = 3169) was performed, based on the minimum within-cluster variance Ward's agglomeration (hclust function; stats package). The number of clusters was determined thanks to the bar heights at one of the most marked jumps (6 clusters). The heatmap and its dendrogram were displayed (heatmap.2 function; stats package). Each peptide cluster was characterized based on a number of qualitative and quantitative physicochemical characteristics (catdes function; FactoMiner package). The qualitative characteristics were the parent protein, the P1 and P1′ cleavage sites. The quantitative characteristics were the molecular weight, the isoelectric point, the peptide length and the number of essential amino acids. Peptide abundances were compared within each cluster using a mixed linear model for repeated measures, with "Time", "Meal" and their interaction as fixed factors and peptide as a random factor. When differences were significant (p-value < 0.05), post hoc tests were performed to test differences among meals at each time point by using a linear contrast analysis adjusted with a Bonferroni correction (glht function; multcomp package).

An in-house program allowed the mapping and the calculation of the average cumulative abundances of the peptides on the parent protein sequence of α_{s1}-casein (CASA1), α_{s2}-casein (CASA2), β-casein (CASB), κ-casein (CASK), α-lactalbumin (LALBA), β-lactoglobulin (LACB) and lactoferrin (TRFL). For each digestion replicate and each digestion phase (undigested, gastric or intestinal samples), abundances of the peptides were averaged over the different digestion times of the corresponding phase, summed amino acid by amino acid and log10-transformed [log10 (abundance + 1)]. Missing abundances were set at 0. This mapping provides a visual overview by heatmap representation of the position of peptides released within the parent protein sequence (heatmap.2 function; stats package).

Identified peptides in undigested, gastric or intestinal samples were examined for homology with literature-identified bioactive peptides using the Biopep Database (March 2020; 3897 sequences; Iwaniak et al., 2016) and the MBPDB Database for lactoferrin-derived peptides (July 2020; 65 sequences; Nielsen et al., 2017). Only exact matching between sequences was considered.

3. Results and discussion

3.1. Structural changes during in vitro gastric digestion

Fig. 1 shows the particle size distributions (Fig. 1A) and the microstructure (Fig. 1B) of the IMFs before and during digestion. Before digestion, the particle size distributions were similar among IMFs, all presenting a main peak at an average mode of 0.15 ± 0.01 μm assigned to the casein micelles.

At G40 (pH 6.2), the protein particle size in the unheated control IMF strongly increased with aggregated protein structures having a 408 ± 66 μm modal diameter. These aggregates were of irregular shape (Fig. 1B). Similar protein particle size increase was observed by Huppertz & Lambers (2020) for IMFs in presence of pepsin and at gastric pH 6.0. It could be explained by the preferential pepsinolysis of the exposed κ-casein, inducing the rapid aggregation of para-casein micelles (Tam & Whitaker, 1972). These protein particles were visible to the naked eye in the gastric compartment as soon as about 20 min of gastric digestion (~pH 6.5) (Supplementary Fig. 1). On the contrary, such particle size increase was not observed for the other studied IMFs indicating that casein micelles aggregation was hindered. The binding of either denatured whey proteins for the heated IMFs (Ferron-Baumy et al., 1991) or lactoferrin for the unheated LF^{+} α-LA^{+} IMF (Anema & de Kruif, 2013) to the surface of casein micelles may alter its surface characteristics and/or the accessibility of κ-casein cleavage sites by pepsin thus delaying its action.

At G80 (pH 5.6), the protein particle size for the unheated IMFs was still very large while that for the heated IMFs had greatly increased, with a modal diameter of 14 ± 1 μm or 21 ± 1 μm for the heated control or LF^{+} α-LA^{+} IMFs, respectively (Fig. 1A). On the opposite, the protein particle size profile was unchanged for the unheated LF^{+} α-LA^{+} IMF. The CLSM images showed a dense distribution of small and compact protein aggregates for the heated control IMF and more linear strands of protein for the heated LF^{+} α-LA^{+} IMF (Fig. 1B). This evolution of the microstructure for the heated IMFs was probably more the consequence of the acid coagulation of the proteins than their destabilization by pepsin. It has been previously reported that casein micelles coated with denatured whey proteins coagulate at higher pH (5.1) than native casein micelles (4.7) (Guyomarc'h et al., 2003). The present protein particle profiles, obtained at the gastric emptying half time, was similar to that previously

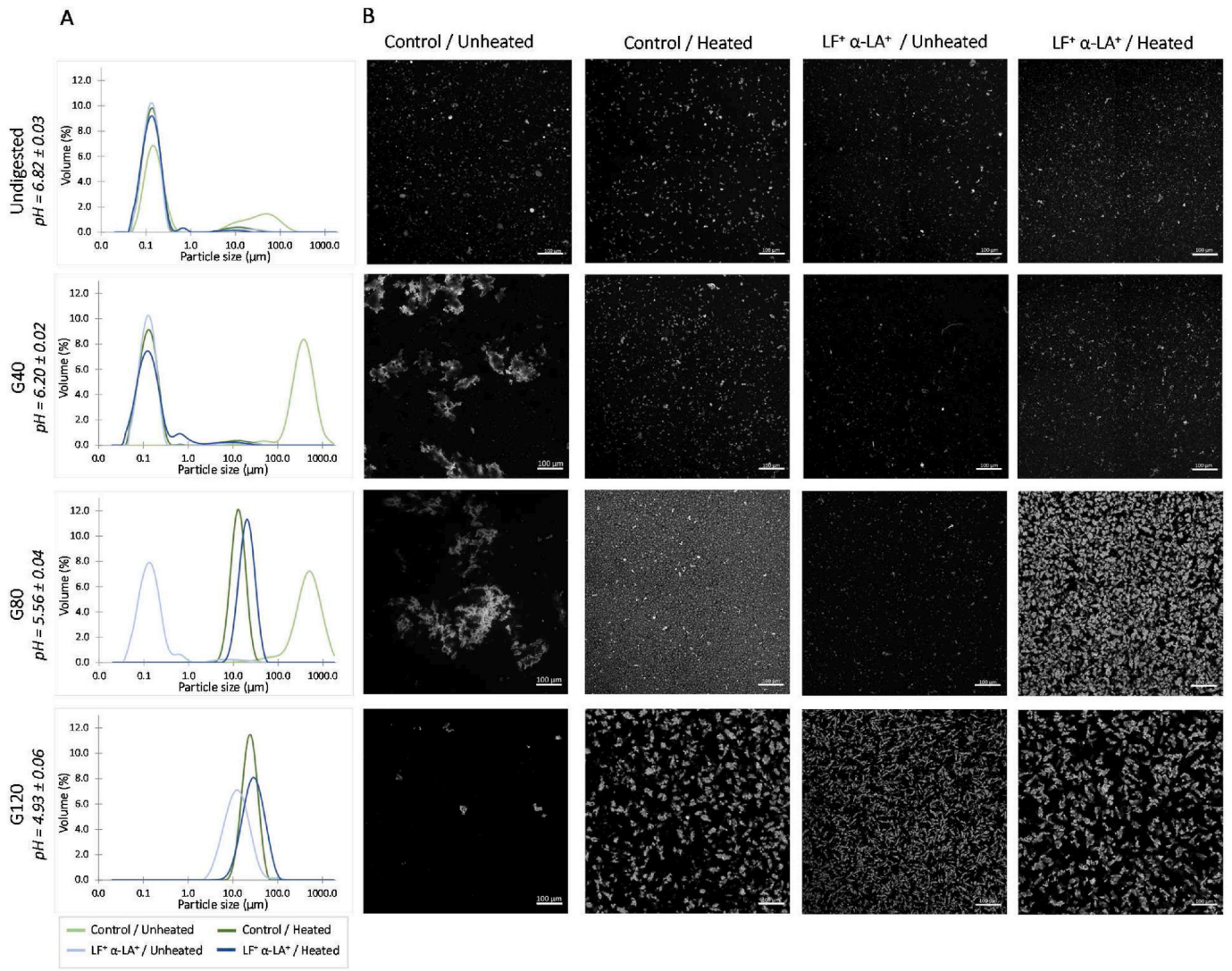

Fig. 1. (A) Particle size distribution profiles and (B) confocal laser scanning microscopy images during the *in vitro* dynamic gastric digestion of IMFs.
(A) Data represent means of three independent digestion experiments (n = 3), with each measurement performed in triplicate. At G120, the protein particle size for the unheated control IMF was too low to be quantified.
(B) Confocal images were observed at a magnification of ×20. Proteins are colored in white (FastGreen®). Scale bar: 100 µm.

observed at the end of the gastric static digestion of the same IMFs (pH 5.3) (Halabi, Croguennec, et al., 2020). This highlights the relevance of the static digestion parameters, initially chosen to mimic the gastric emptying half time (Ménard et al., 2018).

At G120 (pH 4.9), the protein particle size for the unheated LF^+ α-LA^+ IMF greatly increased compared to that at G80 to get closer to that for the heated IMFs (13 ± 1 µm). Besides pepsinolysis impact, this can be explained by the decrease of the net charge of the remaining casein micelles, thus reducing their electrostatic interactions with lactoferrin, and leading to casein coagulation (Anema, 2019). On the contrary, the protein particle profile of the heated IMFs remained unchanged, while the protein particle size for the unheated control IMF could not be quantified due to a low material density, as observed by CLSM analysis.

3.2. Protein hydrolysis during in vitro gastrointestinal digestion

3.2.1. Residual intact proteins

The kinetics of disappearance of the intact proteins, namely caseins, α-lactalbumin, β-lactoglobulin and lactoferrin, were observed by SDS-PAGE under reducing conditions (Fig. 2A, Supplementary Fig. 2). By comparison with the proportion of meal remaining in the total digesta volume (meal + secretions), set up to be the same for all IMFs, it can be deduced whether the protein disappearance was only due to dilution by secretions and emptying or was additionally due to hydrolysis.

Whatever the IMFs, the caseins were rapidly hydrolyzed during the gastric digestion with no intact caseins remaining at the end of the gastric digestion. At G80, the casein hydrolysis tended to be reduced for the unheated control IMF compared to the heated control IMF (p-value = 0.0503), which was explained by the presence of large protein aggregates in the gastric compartment at this time (Fig. 1A), reducing the surface area accessible for pepsin action and/or limiting the pepsin diffusion into the clot (Ye et al., 2016). For similar reason, a high sampling heterogeneity was observed for the unheated control IMF at G80 and only two out of three samples could be considered for SDS-PAGE analysis (Supplementary Fig. 1). Nevertheless, the present result is in agreement with what was observed during the static digestion of the same IMFs (Halabi, Croguennec, et al., 2020). At G120, a treatment effect was observed only for the LF^+ α-LA^+ IMFs with 2 ± 0% *vs.* 9 ± 5% of residual caseins for the unheated or heated LF^+ α-LA^+ IMFs, respectively. This could be linked to the slightly higher size (x 2.5) of the protein aggregates in the heated LF^+ α-LA^+ IMF (Fig. 1A).

During the gastric digestion, β-lactoglobulin appeared to be resistant

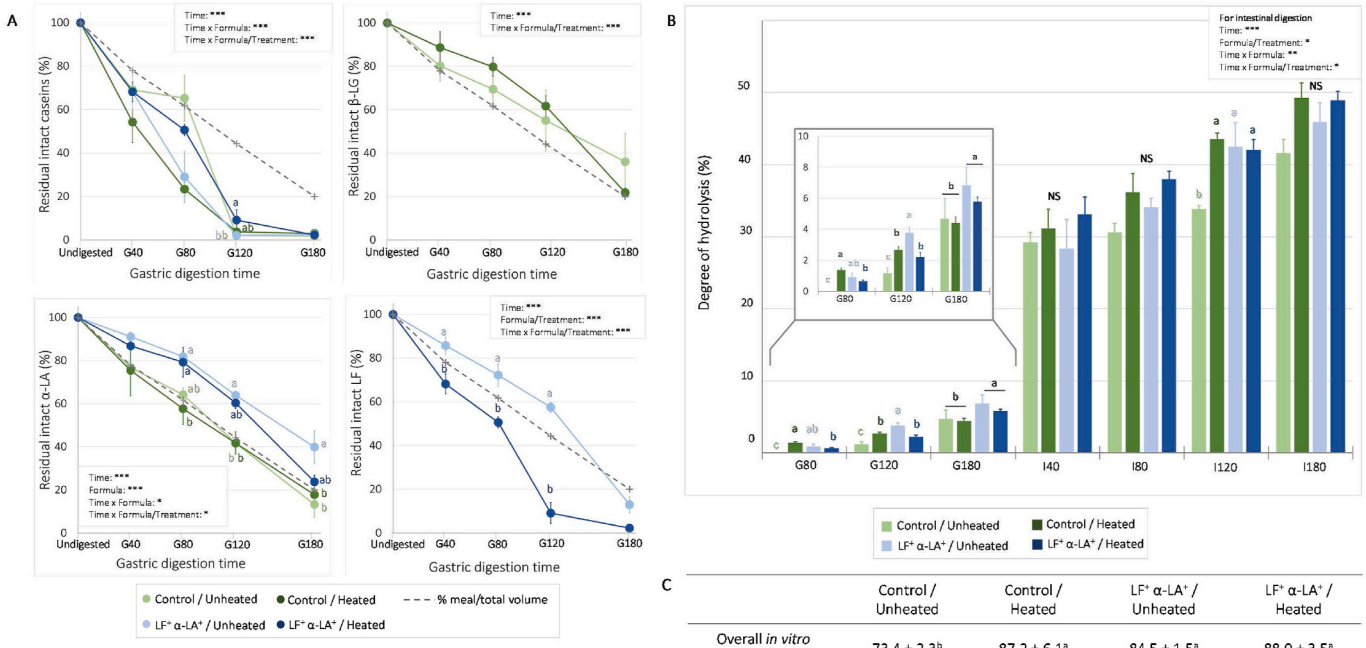

C

	Control / Unheated	Control / Heated	LF⁺ α-LA⁺ / Unheated	LF⁺ α-LA⁺ / Heated
Overall *in vitro* digestibility (%)	73.4 ± 2.3^{b}	87.2 ± 6.1^{a}	84.5 ± 1.5^{a}	88.0 ± 3.5^{a}
Instantaneous *in vitro* digestibility (%)	95.3 ± 4.3^{ns}	91.9 ± 5.9^{ns}	86.2 ± 1.5^{ns}	92.4 ± 2.8^{ns}

Fig. 2. (A) Proportions of residual caseins and major whey proteins as determined by SDS-PAGE analysis and (B) evolution of the degree of hydrolysis during the *in vitro* dynamic gastrointestinal digestion of IMFs and (C) overall or instantaneous *in vitro* digestibility at the end of intestinal digestion of IMFs.
Statistically significant factors were referenced with $p < 0.001$ (***), $p < 0.01$ (**), $p < 0.05$ (*) and $p > 0.05$ (NS). Different superscript letters for a given digestion time represent significant difference among treatments nested within formulas ($p < 0.05$). Data from undigested IMFs were not included in the statistical analysis. (A) Data are means ± SD (n = 3), except for remained casein data at G80, where n = 2 due to one non-representative sampling. Data for residual caseins were log-transformed to respect the hypotheses of residual normality and variance homogeneity (BoxCox transformation) required for the analysis of variance. (B) Data are means ± SD (n = 3), with each measurement performed in triplicate. Statistical analysis was conducted time per time for gastric samples as boxcox transformation was not sufficient to respect the residual normality and the variance homogeneity. (C) Data are means ± SD (n = 3), with each measurement performed in duplicate. Instantaneous *in vitro* digestibility data were transformed as the inverse of the square data to respect the hypotheses of residual normality and variance homogeneity (BoxCox transformation) required for the analysis of variance. Different superscript letters for a given digestibility category represent significant difference among treatments nested within formulas ($p < 0.05$). ns: $p > 0.05$.

to pepsin hydrolysis in a similar manner for the unheated and heated control IMFs; however, the peptide release was different, as discussed below. A significant difference appeared regarding the kinetics of the α-lactalbumin band disappearance between the control IMFs and the LF^{+} α-LA^{+} IMFs, but this was likely due to the co-elution of lactoferrin-derived peptides on the track of the LF^{+} α-LA^{+} IMFs gastric digest, as determined by mass spectrometry analysis after trypsinolysis of the corresponding protein band (data not shown). Similar resistance of the intact whey proteins to pepsin hydrolysis was observed for the same IMFs under static conditions (Halabi, Croguennec, et al., 2020), as well as for raw or pasteurized human milk (de Oliveira et al., 2016). No more intact β-lactoglobulin or α-lactalbumin were observed during the intestinal digestion on the SDS-PAGE.

Lactoferrin was resistant to pepsin hydrolysis during the entire gastric digestion for the unheated LF^{+} α-LA^{+} IMF, unlike that for the heated LF^{+} α-LA^{+} IMF. These results are in accordance with our previous study conducted under static conditions (Halabi, Croguennec, et al., 2020), as well as with studies conducted on raw *versus* pasteurized human milk using the same dynamic system (Nebbia et al., 2020; De Oliveira et al., 2016). The resistance of native lactoferrin to pepsinolysis could be explained by its globular structure (Halabi, Croguennec, et al., 2020), which remained stable despite the pH decrease. In contrast, denatured/aggregated lactoferrin, for which the extent of denaturation was 98% for the heated LF^{+} α-LA^{+} IMF (Supplementary Table 1), was much more prone to pepsin hydrolysis, likely due to a more flexible conformation and better accessibility to the cleavage sites (Stănciuc et al., 2013). However, the hydrolysis kinetics was much slower with the present dynamic conditions than with the static ones (Halabi, Croguennec, et al., 2020), with a time required to reach about 80% of hydrolysis of the intact lactoferrin of 120 min vs. 5 min, respectively. This was linked to the progressive pH decrease, which delayed the pepsin activity and progressively induced changes in the less stabilized structure of the denatured/aggregated lactoferrin (Sreedhara et al., 2010). Overall, as discussed previously (Halabi, Croguennec, et al., 2020), the bioactive properties of LF are likely to be impacted not only by the heat-induced conformational changes but also by the subsequent greater pepsinolysis. This, however, remains to be demonstrated.

Interestingly, the kinetics of lactoferrin disappearance for the heated LF^{+} α-LA^{+} IMF was very similar to that of caseins in the same IMF, suggesting that pepsin hydrolyzed similarly both proteins within the lactoferrin-caseins aggregates. A slight electrophoretic band at ~50 kDa was observed at G120 and G180 only for the unheated LF^{+} α-LA^{+} IMF. This protein band, assimilated to the C-terminal fragment of lactoferrin (Sharma et al., 2013), was still present during the intestinal digestion and appeared to be resistant to intestinal enzymes, as previously reported (Rastogi et al., 2014). In addition, in the same IMF, some intact lactoferrin was observed in the early digestion time as well as a band at ~37 kDa. This band, only observed in the unheated LF^{+} α-LA^{+} IMF, could be another product of lactoferrin hydrolysis.

An electrophoretic band for BSA was observed only for the control IMFs but it could not be quantified due to its low intensity. This band decreased progressively during the gastric digestion in a slower manner for the unheated control IMF, for which some intact BSA was still observed during intestinal digestion.

3.2.2. Degree of hydrolysis and protein digestibility

Fig. 2.B shows the DH evolution during *in vitro* gastrointestinal digestion. During the gastric digestion, the DH slightly increased for all IMFs to reach at 180 min values of 5 ± 1% for the control IMFs vs. 6 ± 1% for the LF^+ α-LA^+ IMFs, in agreement with those obtained by Le Roux, Menard, et al. (2020).

In the intestinal compartment, proteolysis drastically increased for all IMFs and reached an average DH of 30 ± 2% at 40 min. Afterwards, the DH progressively increased for all IMFs ($p < 0.05$) but in a different manner, with a DH tending to be lower for the unheated control IMF than for the other IMFs, this difference being statistically significant only at 120 min. DH did not significantly differ among IMFs at 180 min and reached 46 ± 4% for all IMFs, value in line with Le Roux, Menard, et al. (2020). The final DH values were 15–28% higher under dynamic than under static conditions for the unheated LF^+ α-LA^+ IMF and the control IMFs. A similar difference has been previously reported between static and dynamic models of digestion applied to a control IMF (Le Roux, Chacon, et al., 2020; Le Roux, Menard, et al., 2020). However, the reverse was true for the heated LF^+ α-LA^+ IMF with a DH being 18% lower under dynamic than under static conditions (Halabi, Croguennec, et al., 2020). This must be due to the slower lactoferrin hydrolysis and its concomitant delivery towards the intestinal compartment under the dynamic conditions (Fig. 2A), while an almost complete hydrolysis of the denatured lactoferrin was observed during the static gastric digestion before being submitted to the intestinal phase.

In vitro protein digestibility was calculated considering all the intestinal digestible N (<10 kDa), such as previously suggested (Moughan, 1999) related to the N content of the meal, the latter being determined either by calculation (overall digestibility) or by analysis of the total N content in the digesta to which was subtracted the estimated N arising from the secretions (instantaneous digestibility) (Fig. 2C). The overall protein digestibility for the unheated control IMF was significantly lower than that for the other IMFs, while the instantaneous digestibility was not significantly different among IMFs (mean value of 91.5 ± 4.8%). The overall and instantaneous digestibility values were in good agreement, except for the unheated control IMF, for which the overall digestibility was lower than the instantaneous digestibility (−22 percentage points), thus revealing an overestimation of the N content of the meal by calculation for this IMF. This indicates that the meal emptying did not occur as theoretically expected. The irregular transit of dietary nitrogen towards the intestinal compartment could be explained by the heterogeneity of the unheated control IMF gastric digest containing large protein particles (Fig. 1B). This suggests that proteins from the unheated control IMF are slowly emptied, which could impact the kinetics of absorption, and further modulate the postprandial regional metabolic fate of nitrogen, at least as demonstrated in adults (Deglaire et al., 2009). The present protein digestibility for the heated control IMF corroborated with that reported for similar IMF digested *in vitro* in Le Roux, Menard, et al. (2020) (89.2 ± 3.9%), but was slightly higher than that reported in Maathuis et al. (2017) (73.4 ± 2.7%). This difference may be due to a lower cut-off size, although not clearly stated.

3.3. Peptide profile during in vitro gastrointestinal digestion

The present peptide release, and more largely the proteolysis pattern, obtained after *in vitro* digestion using porcine enzymes, is expected to be a good approximation of what would be obtained in human infants, as the pig, including the piglet, is recognized as a good animal model of

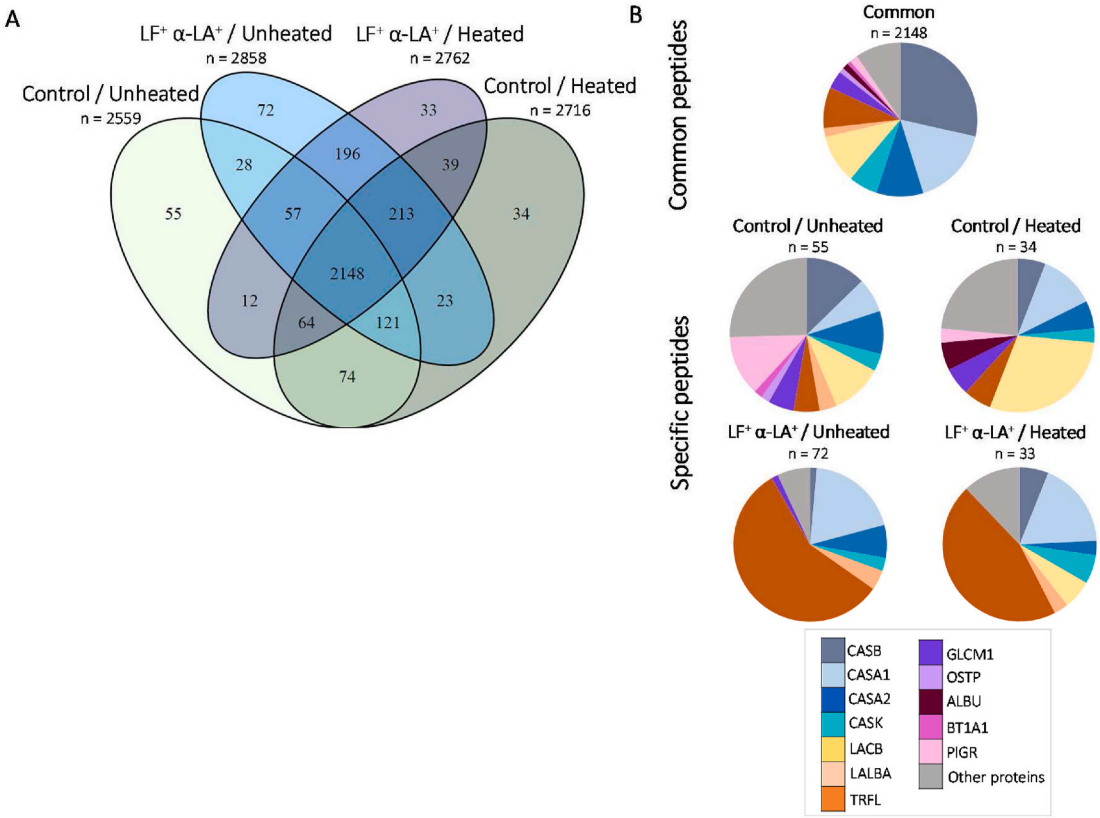

Fig. 3. (A) Venn diagram of peptides and (B) parent protein of the common and specific peptides during the *in vitro* dynamic gastrointestinal digestion of IMFs. (A) n values correspond to the peptide amounts. Venn diagram was created with all the identified peptides before digestion and released during the *in vitro* dynamic gastrointestinal digestion of the IMFs. (B) Abbreviations are CASA1: α_{s1}-casein, CASA2: α_{s2}-casein, CASB: β-casein, CASK: κ-casein, LACB: β-lactoglobulin, LALBA: α-lactalbumin, TRFL: lactoferrin, GLCM1: glycosylation-dependent cell adhesion molecule 1, OSTP: osteopontin, ALBU: albumin, BT1A1: Butyrophilin Subfamily 1 Member A1, PIGR: Polymeric immunoglobulin receptor. Peptides were identified against the « Bos Taurus » protein database (6 905 proteins; source: https://uniprot.org).

human for studying protein digestion (Darragh et al., 1995; Deglaire et al., 2009). More specifically, a previous study has shown that a similar peptide profile was obtained after milk protein digestion either *in vivo*, in humans, or *in vitro*, using porcine enzymes (Sanchòn et al., 2018).

3.3.1. Peptide identification

Prior to and during digestion of the IMFs, a total of 3169 unique peptides of 6–50 amino acids were identified (data available at https://doi.org/10.15454/6OTI1M), with 2148 peptides common among the IMFs (Fig. 3A). The majority of the identified peptides derived from caseins (61%) and to a minor extent from the major whey proteins (21%) (Fig. 3B), as previously reported for IMFs (Hodgkinson et al., 2019). More precisely, a great proportion of the identified peptides originated from β-casein (29% of the total unique peptides), as previously reported for IMFs (Wada et al., 2017) or human milk (Deglaire et al., 2019). Regarding the whey proteins, 10% of total unique peptides derived from β-lactoglobulin, 9% from lactoferrin and 2% from α-lactalbumin. The low number of peptides originating from whey proteins could reflect the resistance of whey proteins to pepsin hydrolysis during the gastric digestion (Fig. 2A), but also probably the non-identification of the peptides linked together by disulphide bonds. Finally, 18% of the common peptides derived from minor proteins. Venn diagram showed that 55 and 34, or 72 and 33 peptides were specific for the unheated and heated control IMFs, or for the unheated and heated LF^+ α-LA^+ IMFs, respectively (Fig. 3A). Specific peptides mainly derived from the minor proteins (47%) for the control IMFs or from lactoferrin (57% and 45% for the unheated and heated LF^+ α-LA^+ IMFs, respectively) for the LF^+ α-LA^+ IMFs.

3.3.2. Peptide clustering and kinetics of peptide release

The clustering analysis grouped the 3169 unique peptides into six clusters (Fig. 4). The parent protein was the variable the most significantly explaining the clustering (p-value = 1.11×10^{-104}) (Supplementary Table 2), such as previously reported (Deglaire et al., 2019). Particularly, peptides from caseins vs. those from lactoferrin and β-lactoglobulin were associated to clusters in an opposite manner.

Clusters 4, 5 and 6 included peptides almost exclusively released during the gastric digestion and represented a large majority (74%) of the identified peptides (Fig. 4B). Cluster 4 included peptides originating mostly from caseins (78% of cluster peptides; 35–48% of the total casein peptides), of which 101 peptides were present before digestion (Fig. 4A) with a slightly higher average abundance in the unheated IMFs, which could partly explain the subsequent greater abundance at G80 for these IMFs. Cluster 5 contained significantly less lactoferrin peptides than in overall, unlike that in cluster 6. The latter presented an average peptide abundance higher in the LF^+ α-LA^+ IMFs than in the control IMFs at G80, linked to the higher lactoferrin content. At G180, the abundance became higher for the heated LF^+ α-LA^+ IMF than for the unheated LF^+ α-LA^+ IMF, likely due to the increased proteolysis of denatured lactoferrin (Fig. 2B). It can be noted that the peptide average release rate between G80 and G180 were similar between the two heated IMFs, in agreement with the SDS-PAGE analysis.

In contrast, clusters 2 and 3 (18% of the total peptides) gathered peptides almost exclusively released during the intestinal digestion (Fig. 4B). The lower proportion of peptides identified in the intestinal phase is likely due to the non-identification of peptides lower than 6 amino acids. Cluster 2 contained the same proportion of casein peptides as in overall. A constantly lower abundance of peptides from the unheated control IMF was observed, which could result from the slower dietary N transfer from gastric to intestinal compartment. In cluster 3, peptides were mainly originating from lactoferrin (33% of the cluster peptides vs. 15% in overall) and β-lactoglobulin (22% of the cluster peptides vs. 11% in overall). The average peptide abundance was significantly lower for the unheated control IMF than in the other IMFs

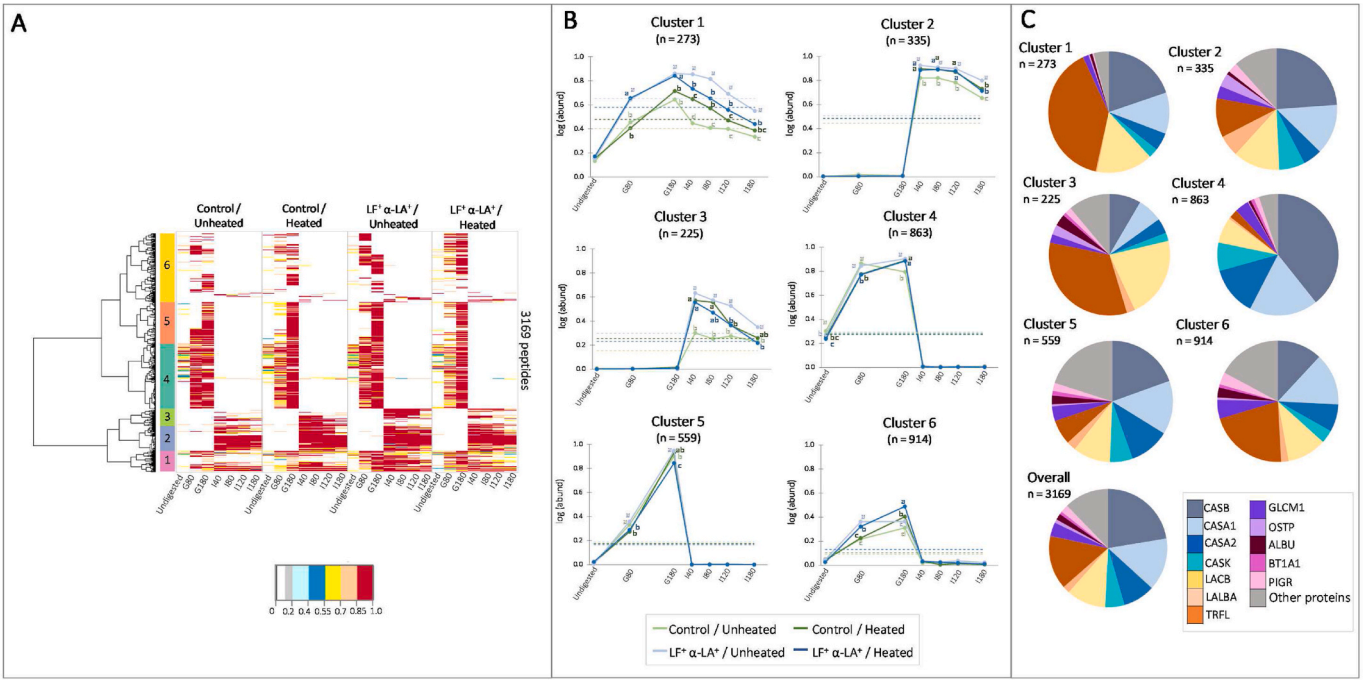

Fig. 4. (A) Heatmap abundances as classified by hierarchical classification and (B) average abundances of the peptides by cluster during the *in vitro* dynamic gastrointestinal digestion of IMFs - (C) parent proteins of the peptides by cluster.
Peptide abundances were log10-transformed followed by setting the maximum abundance to 1. (A) White stretches indicate regions where no peptides were identified. Blue color indicates low abundance graduating to red color for high abundance of peptide identified. (B) the dashed-pointed curves represent the mean kinetics for each IMFs. Different superscript letters for a given digestion time represent significant difference among meals ($p < 0.05$). (C) Abbreviations are CASA1: α_{s1}-casein, CASA2: α_{s2}-casein, CASB: β-casein, CASK: κ-casein, LACB: β-lactoglobulin, LALBA: α-lactalbumin, TRFL: lactoferrin, GLCM1: glycosylation-dependent cell adhesion molecule 1, OSTP: osteopontin, ALBU: albumin, BT1A1: Butyrophilin Subfamily 1 Member A1, PIGR: Polymeric immunoglobulin receptor. Overall peptides correspond to peptides within the entire dataset.

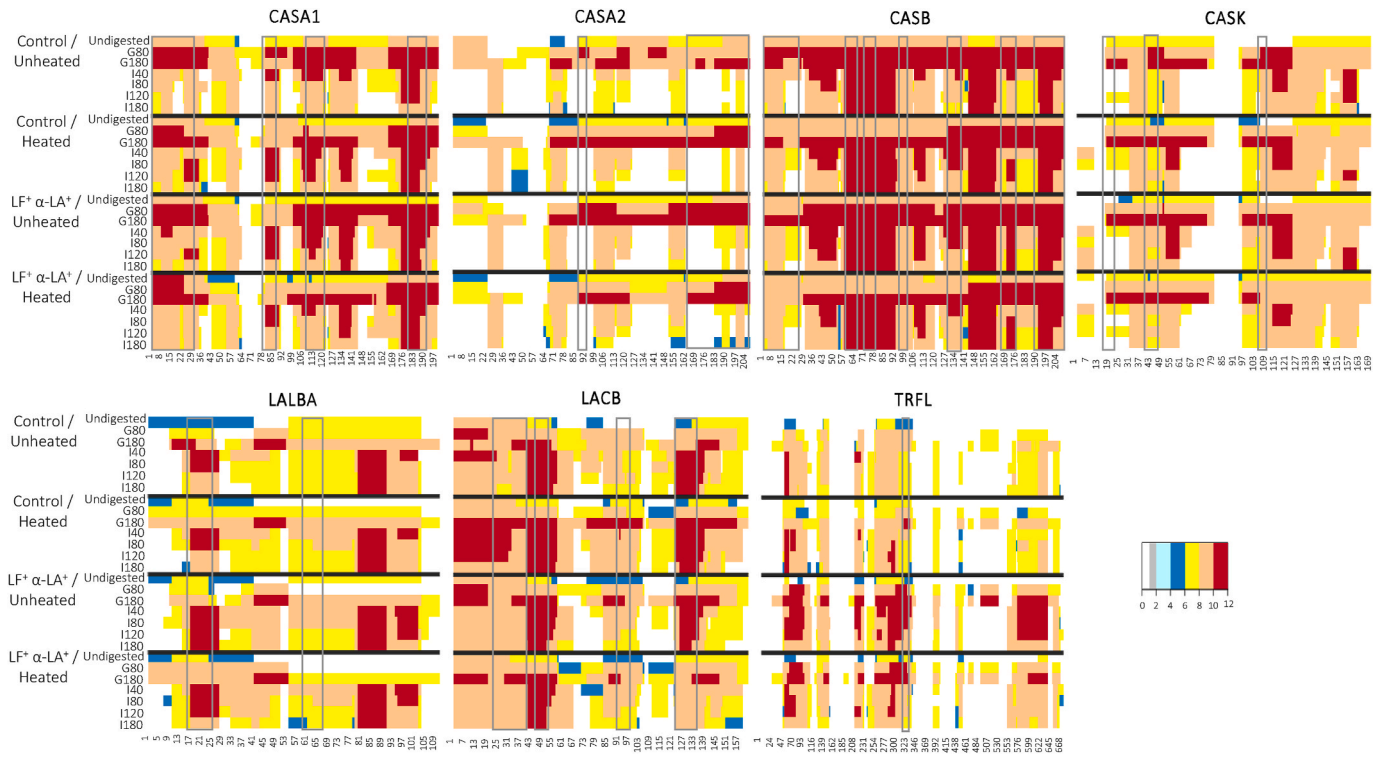

Fig. 5. Mapping on the sequence of the major parent proteins of the peptides released during the *in vitro* dynamic gastrointestinal digestion of IMFs. Abbreviations are CASA1: α_{s1}-casein, CASA2: α_{s2}-casein, CASB: β-casein, CASK: κ-casein, LACB: β-lactoglobulin, LALBA: α-lactalbumin, TRFL: lactoferrin. Peptide abundances, summed at each amino acid, were log10-transformed. The x-axis represents the amino acid sequence of parent protein and the y-axis represents the digestion time for each IMFs. White stretches indicate regions where no peptides were identified. Blue color indicates low abundance graduating to red color for high abundance of amino acid identification within the protein sequence. The boxed areas correspond to areas where bioactive peptides have been identified using BIOPEP and MBPDB databases.

except at the end point. This could be partially linked to a slower hydrolysis of the native β-lactoglobulin, such as reported by Nicoleta et al. (2008). Conversely, the peptide abundance was significantly higher for the unheated LF^+ α-LA^+ IMF, likely due to the digestive resistance of the peptides coming from native lactoferrin, as shown by SDS-PAGE analysis (Fig. 2B). These different intestinal peptide abundances from lactoferrin and β-lactoglobulin depending on their heat treatment could be observed on the peptidomic profiles of these proteins (Fig. 5).

Finally, cluster 1 (9% of the total peptides) included peptides released during the gastric phase as well as during the intestinal phase (Fig. 4A). Cluster 1 was mainly associated to lactoferrin and β-lactoglobulin. The average gastric abundances for cluster 1 was significantly higher for the LF^+ α-LA^+ than for the control IMFs, likely due to their higher lactoferrin content. Different kinetics of intestinal peptide release were observed across all the IMFs in a similar trend to that for cluster 3, probably linked to the different hydrolysis susceptibility of native vs. heat-denatured β-lactoglobulin and lactoferrin.

3.3.3. *Peptidomic profiles of the major proteins during the gastrointestinal digestion of IMFs*

Fig. 5 shows the cumulative abundance of the peptides mapped onto the sequence of the major proteins during digestion. As stated above, the peptide abundance from β-casein was high and covered the entire sequence almost during the entire digestion. Some specific regions of the sequence were never covered by any peptide and in any IMF for κ-casein and to a greater extent for lactoferrin.

In all IMFs, peptides in the 57–93, 142–163 and 192–209 regions of β-casein that have high proportion of proline residues were highly abundant during digestion, as previously observed for bovine milk (Dupont et al., 2010; Sánchez-Rivera et al., 2015). Some peptide release kinetics were different between the heated and unheated IMFs. Particularly, at G80, the cumulative peptide abundance in the regions 28–128 or 28–142 was higher for the unheated control and LF^+ α-LA^+ IMFs, respectively, than for the heated IMFs, which can partly explain the higher overall abundance observed in cluster 4 for these IMFs. Based on the kinetics profile of the gastric phase, this can be interpreted as a faster hydrolysis of these regions in the unheated IMFs. This could be linked to the absence of whey protein aggregates at the surface of the casein micelles (Halabi, Deglaire, Hennetier, et al., 2020), thus allowing an easier access of pepsin, at least at the outer surface of the micelle aggregates formed during digestion, such as in the unheated control IMF (Fig. 1). In the intestinal phase, peptides from the region 30–56 were more abundant during the first 2 h of intestinal digestion, and thus more resistant to further hydrolysis, for the unheated LF^+ α-LA^+ IMF compared to the other IMFs. This was in accordance with the results of Sánchez-Rivera et al. (2015) who compared raw vs. heated bovine milk. Whether this is induced by the interaction between native and undigested lactoferrin with casein micelles remains unknown. Interestingly, peptides from the bioactive region 170–176 were more abundant during the whole intestinal digestion for the unheated LF^+ α-LA^+ IMF compared to the other IMFs.

For α_{s1}-casein, peptides from the 24–40 and 99–142 regions were, at G80, more abundant for the unheated IMFs compared to the heated IMFs, such as observed for β-casein. This can also contribute to the higher abundance observed in cluster 4. As explained for β-casein, this may be linked to the binding of whey protein aggregates onto the casein micelles, thus hindering the pepsin action. During the intestinal digestion, peptides in the bioactive region 110–121 were more resistant to hydrolysis in the unheated LF^+ α-LA^+ IMF than in the other IMFs, which, interestingly, has been observed in raw vs. pasteurized human milk during *in vitro* dynamic intestinal digestion (Deglaire et al., 2019).

For α_{s2}-casein, peptides from the regions 89–114 and 151–183 were

more abundant, at G80, solely for the unheated LF^+ α-LA^+ IMF, while at the end of gastric digestion, peptides from the larger region 69–207, were still more abundant for the unheated LF^+ α-LA^+ IMF but also for the heated control IMF. In the intestinal digestion, the 1–24, 36–65 (except for the heated control IMF), 81–98, 125–149 and 163–182 regions of α_{s2}-casein had no sequence coverage during the intestinal digestion of IMFs, although most of these regions were covered by the end of the gastric phase. Thus, this could indicate that these regions were rapidly hydrolyzed during the intestinal phase.

For κ-casein, peptides were mainly identified in the regions 18–75 and in the region 96–124 at the end of gastric digestion. The region between 75 and 96 had no peptide along the entire digestion due to the presence of an inter-molecular disulfide bond. At G80, a higher abundance was observed in the regions 43–18 and 109–127 solely for the unheated control IMF. This could result from the preferential pepsinolysis of the exposed κ-casein, as stated above, and responsible of the rapid aggregation of para-casein micelles and thus of the larger aggregates observed during digestion (Fig. 1). During the intestinal digestion, the abundance was higher for the unheated LF^+ α-LA^+ IMF during the first 2 h of digestion in some specific regions (52–59 and 113–124), such as observed for β-casein. As stated above, whether this is induced by the interaction between native and undigested lactoferrin with casein micelles remains unknown.

Regarding the whey proteins, it can be noted that for α-lactalbumin, prior to digestion, peptides in the region 41–110 were identified solely in both unheated IMFs. Intestinal peptides were more abundant in the bioactive region 17–27 and in the region 96–102 for the LF^+ α-LA^+ IMFs than for the control IMFs, which can result from the higher content of α-lactalbumin in the LF^+ α-LA^+ IMF.

For β-lactoglobulin, peptides in the region 106–120 were released earlier (G80) in the heated formulas than in the unheated ones and at the end of gastric digestion, peptide abundance in the regions 1–32, 74–104 and 123–156 was higher for the heated than for the unheated control IMF. This could indicate a higher hydrolysis level of denatured β-lactoglobulin, although this was not visible at the protein level as observed by SDS-PAGE (Fig. 2A). During intestinal digestion, a higher peptide abundance was still observed for the region 1–32 particularly for the heated control IMF, which also included a bioactive area. This can partly explain the higher abundance observed in cluster 3. Whether this is due to a greater hydrolysis of the denatured β-lactoglobulin, such as suggested previously (Nicoleta et al., 2008), or whether, on the contrary, to protein resistance due to the formation of β-lactoglobulin aggregates remains unknown. In both cases, this may be linked to the trypsin accessibility towards the lysine residues within the regions 17–39 (Zenker et al., 2020).

Peptides derived from lactoferrin did not entirely cover the lactoferrin sequence during the digestion of IMFs, with many blank regions (i.e. 1-51, 153–208, 336–383, 399–440, 450–559 and 641–650), as previously shown for human milk (Deglaire et al., 2019). This could be explained by the presence of seventeen disulphide bonds stabilizing bovine lactoferrin structure, making the peptide detection by LC-MS/MS highly challenging. As expected, the peptide abundance was greater in the LF^+ α-LA^+ IMFs than in the control IMFs. Unlike observed by SDS-PAGE analysis (Fig. 2A), the higher gastric hydrolysis of LF was not evidenced here. It should be noted that, unlike for the other proteins, each peptide identified represented at the maximum 7% of the lactoferrin sequence; thus, large peptides, responsible of the different LF gastric hydrolysis, may not have been identified here. During intestinal digestion, the cumulative peptide release was more abundant for the unheated LF^+ α-LA^+ IMF than for the heated LF^+ α-LA^+ IMF in the regions 52–96, 209–222, 283–327 and 572–640, which reflected the higher resistance of the native lactoferrin to gastrointestinal digestion, such as reported above (Fig. 2A and Fig. 4B).

3.3.4. *Bioactive peptide release during the in vitro intestinal digestion*

Bioactive peptides released during the gastric digestion are presented in Supplementary Table 3. Briefly, 37 bioactive peptides were identified during the gastric digestion, with about half of them originating from α_{s2}-casein (16), and a minor part from β-casein (8) and α_{s1}-casein (7). The majority of these peptides had antimicrobial and angiotensin converting enzyme (ACE) inhibitor properties, as observed by Hodgkinson et al. (2019) during the infant *in vitro* gastric digestion of bovine milk. In contrast, no bioactive peptides derived from α-lactalbumin or lactoferrin were identified.

During the intestinal digestion (Table 1), a higher number of bioactive peptides was identified for the LF^+ α-LA^+ IMFs (25) than for the control IMFs (19), due to a greater number of casein-derived bioactive peptides. Among the identified bioactive peptides, 9 of them, mainly originating from caseins, were generated during the gastric digestion and were still present during the intestinal digestion (Supplementary Table 3 and Table 1). These casein-derived peptides had at least one proline residue in their sequence, possibly explaining their

Table 1
Bioactive peptides identified during the *in vitro* dynamic intestinal digestion of IMFs.

Parent protein [1]	Peptide position [2]	Peptide sequence [3,4]	Activity	Abundance [5]											
				Control / Unheated				Control / Heated				LF^+ α-LA^+ / Unheated				LF^+ α-LA^+ / Heated			
				I40	I80	I120	I180	I40	I80	I120	I180	I40	I80	I120	I180	I40	I80	I120	I180
CASA1	1-23	RPKHPIKHQGLPQEVLNENLLRF	Immunomodulating; Antibacterial; Antiviral																
	80-90	HIQKEDVPSER	Antioxidative																
	110-121	EIVPNSAEERLH	ACE inhibitor																
	180-193	SDIPNPIGSENSEK	Antibacterial																
CASA2	183-207	VYQHQKAMKPWIQPKTKVIPYVRYL	Haemolytic; Antibacterial; Campde inhibitor																
CASB	60-68	YPFPGPIPN	ACE inhibitor																
	73-82	NIPPLTQTPV	ACE inhibitor																
	98-105	VKEAMAPK	Antioxidative																
	133-139	LHLPLPL	ACE inhibitor																
	134-139	HLPLPL	Antiamnestic																
	170-176	VLPVPQK	Antioxidative																
	191-209	LLYQEPVLGPVRGPFPIIV	Immunomodulating																
	194-206	QEPVLGPVRGPFP	ACE inhibitor																
	202-209	RGPFPIIV	ACE inhibitor																
CASK	31-37	VLSRYPS	Antioxidative																
	42-49	YYQQKPVA	Antibacterial																
	51-60	INNQFLPYPY	Dipeptidyl peptidase IV inhibitor																
	106-111	MAIPPK	Antithrombotic																
LACB	33-42	DAQSAPLRVY	ACE inhibitor																
	92-100	VLVLDTDYK	Antibacterial; Dipeptidyl peptidase IV inhibitor																
	125-135	TPEVDDEALEK	Dipeptidyl peptidase IV inhibitor																
	142-148	ALPMHIR	ACE inhibitor																
LALBA	17-26	GYGGVSLPEW	Dipeptidyl peptidase IV inhibitor																
	61-68	CKDDQNPH	Antibacterial																
TRFL	325-340	DLIWKLLSKAQEKFGK	Antibacterial																

resistance to enzymatic hydrolysis (Sanchón et al., 2018). However, it should be noted that brush border peptidases, including proline-specific peptidases, were not included in our digestion model (Picariello et al., 2015).

The kinetics of bioactive peptide release during the intestinal digestion differed from one peptide to another and among IMFs, which presented 16 bioactive peptides in common. All bioactive peptides from α_{s1}-casein and one from β-casein f(170–176) were more abundant and more resistant in the unheated LF^+ α-LA^+ IMF than in the other IMFs. In addition, the sole bioactive peptide from α_{s2}-casein (i.e. α_{s2}-casein f (183–207)) was solely present in the LF^+ α-LA^+ IMFs (Table 1).

β-casein f(134–139) was abundantly released since the early intestinal digestion time for the unheated control IMF, and then progressively hydrolyzed, while the opposite was true for the heated control IMF. β-casein f(191–209), identified only in the LF^+ α-LA^+ IMFs, was more resistant in the corresponding heated IMF, while the opposite was true for κ-casein f(51–60).

β-lactoglobulin f(92–100) was more abundant and more resistant in the heated control IMF compared to the other IMFs, such as for β-lactoglobulin f(125–135), in accordance with Picariello et al. (2010), who reported that this peptide had a high allergenic potential due to its high resistance to hydrolysis during digestion. On the contrary, β-lactoglobulin f(142–148) was more resistant in the heated LF^+ α-LA^+ IMF than in the corresponding unheated IMF and the heated control IMF.

α-lactalbumin f(61–68) was identified earlier but was hydrolyzed sooner for the unheated LF^+ α-LA^+ IMF as compared to the unheated control IMF. This peptide was not identified in the heated IMFs, except at the last intestinal time for the heated LF^+ α-LA^+ IMF.

Only one bioactive peptide deriving from lactoferrin (fragment 325–340) was identified for the unheated LF^+ α-LA^+ IMF during the first times of intestinal digestion. The low number of bioactive peptides originating from lactoferrin, in line with Deglaire et al. (2019) for human milk digestion, could be linked to the low number of such peptides yet identified in the literature (65 identified peptides in the MBPDB database) (Nielsen et al., 2017), and the presence of disulphide bonds in lactoferrin sequence.

Although the present bioactive peptides have been determined thanks to the BIOPEP database, i.e. based on scientific studies and not on sequence prediction, some limits still need to be kept in mind. First, the bioactive peptides need to reach their site of action as intact, that is with no further hydrolysis. No peptidase from the brush border was included in the present model, which can be a limitation. Secondly, if the site of action is in the inner side of the body, the peptide has to be absorbed through the epithelium. This may occur more easily in the infant as the intestinal permeability is high and decreases progressively while the infant is growing.

4. Conclusion

The present study showed that the protein structures within IMFs generated by varying the IMF protein profile and the heating conditions impacted the digestive kinetics of proteolysis particularly for caseins and lactoferrin. The present model highlighted the importance of the dynamic digestive parameters on the proteolysis kinetics, which was slowed down compared to our previous static study.

The gastric protein coagulation was markedly dependent on the casein micelle structure within IMFs, with large-size protein particles formed in the early period of gastric digestion for IMF that contain native casein micelles (unheated control IMF). As a result, the resistance of caseins upon gastric digestion tended to increase and the nutrient delivery to the intestinal compartment was delayed. In contrast, compact protein aggregates were formed for IMFs containing casein micelle-bound whey proteins in the middle of gastric digestion and low-size protein particles were observed for IMF containing partially disintegrated casein micelles in the latter period of gastric digestion. While α-lactalbumin and β-lactoglobulin exhibit similar resistance to gastric hydrolysis in their native and denatured forms by SDS-PAGE, the susceptibility of lactoferrin to pepsin was significantly enhanced after heat-denaturation. The impact of the protein structures within IMF on the peptidome release was evidenced, particularly on the peptide clusters significantly associated either to caseins or to lactoferrin and β-lactoglobulin. A slower release of intestinal peptides from the IMF containing native casein micelles was observed, on the contrary to the greater peptide resistance of the IMF containing native lactoferrin. Bioactive peptides were more abundant for the IMFs having a whey protein profile close to that of human milk, and particularly for the unheated IMF, due to a greater number of casein-derived bioactive peptides. This may have physiological relevance for the infants. Further studies are required to evaluate whether these peptides would resist the action of the brush border enzymes and if they could pass through the epithelium barrier to reach their targets.

Declaration of interest

The authors declare that they have no known competing financial interests or personal relationships that could have appeared to influence the work reported in this paper.

Author statement

Amira Halabi: Investigation, Writing – Original Draft; Thomas Croguennec, Amélie Deglaire, Saïd Bouhallab, Didier Dupont: Supervision, Writing – Review & Editing; Olivia Ménard, Valérie Briard-Bion, Julien Jardin, Yann Le Gouar, Marie Hennetier: Investigation.

Acknowledgements

We would like to thank Ingredia Dairy Experts and Agropur Inc in providing lactoferrin and α-lactalbumin powders used for the study and Jordane Ossemond for his technical support. This work was supported by the Brittany Region, France (Grant ARED 17-032) and the Institut National de Recherche pour l'Agriculture, l'Alimentation et l'Environnement (INRAE, France).

Appendix A. Supplementary data

Supplementary data to this article can be found online at https://doi.org/10.1016/j.foodhyd.2021.107368.

References

Anema, S. (2019). Acidification of lactoferrin-casein micelle complexes in skim milk. *International Dairy Journal, 99*, 104550. https://doi.org/10.1016/j.idairyj.2019.104550

Anema, S. G., de Kruif, C. G., & Kees). (2013). Protein composition of different sized casein micelles in milk after the binding of lactoferrin or lysozyme. *Journal of Agricultural and Food Chemistry, 61*(29), 7142–7149. https://doi.org/10.1021/jf401270h

Bourlieu, C., Ménard, O., Bouzerzour, K., Mandalari, G., Macierzanka, A., Mackie, A. R., & Dupont, D. (2014). Specificity of infant digestive conditions: Some clues for developing relevant in vitro models. *Critical Reviews in Food Science and Nutrition, 54*(11), 1427–1457. https://doi.org/10.1080/10408398.2011.640757

Brodkorb, A., Egger, L., Alminger, M., Alvito, P., Assunção, R., Ballance, S., Bohn, T., Bourlieu-Lacanal, C., Boutrou, R., Carrière, F., Clemente, A., Corredig, M., Dupont, D., Dufour, C., Edwards, C., Golding, M., Karakaya, S., Kirkhus, B., Le Feunteun, S., … Recio, I. (2019). INFOGEST static in vitro simulation of gastrointestinal food digestion. *Nature Protocols, 14*(4), 991–1014. https://doi.org/10.1038/s41596-018-0119-1

Darragh, A. J., & Moughan, P. J. (1995). The three-week-old piglet as a model animal for studying protein digestion in human infants. *Journal of Pediatric Gastroenterology and Nutrition, 21*(4), 387–393.

Davis, A. M., Harris, B. J., Lien, E. L., Pramuk, K., & Trabulsi, J. (2008). α-Lactalbumin-rich infant formula fed to healthy term infants in a multicenter study: Plasma

essential amino acids and gastrointestinaltolerance. *European Journal of Clinical Nutrition, 62*(11), 1294–1301. https://doi.org/10.1038/sj.ejcn.1602848

Deglaire, A., Bos, C., Tomé, D., & Moughan, P. J. (2009). Ileal digestibility of dietary protein in the growing pig and adult human. *British Journal of Nutrition, 102*(12), 1752–1759. https://doi.org/10.1017/S0007114509991267. Cambridge Core.

Deglaire, A., Oliveira, S. D., Jardin, J., Briard-Bion, V., Kroell, F., Emily, M., Ménard, O., Bourlieu, C., & Dupont, D. (2019). Impact of human milk pasteurization on the kinetics of peptide release during in vitro dynamic digestion at the preterm newborn stage. *Food Chemistry, 281*, 294–303. https://doi.org/10.1016/j.foodchem.2018.12.086

Dupont, D., Boutrou, R., Menard, O., Jardin, J., Tanguy, G., Schuck, P., Haab, B. B., & Leonil, J. (2010). Heat treatment of milk during powder manufacture increases casein resistance to simulated infant digestion. *Food Digestion, 1*(1–2), 28–39. https://doi.org/10.1007/s13228-010-0003-0

Egger, L., Ménard, O., Baumann, C., Duerr, D., Schlegel, P., Stoll, P., Vergères, G., Dupont, D., & Portmann, R. (2019). Digestion of milk proteins: Comparing static and dynamic in vitro digestion systems with in vivo data. *The 5th International Conference on Food Digestion, 118*, 32–39. https://doi.org/10.1016/j.foodres.2017.12.049

Ferron-Baumy, C., Maubois, J. L., Garric, G., & Quiblier, J. P. (1991). Coagulation présure du lait et des rétentats d'ultrafiltration. Effets de divers traitements thermiques. *Le Lait, 71*(4), 423–434. https://doi.org/10.1051/lait:1991432

Guyomarc'h, F., Queguiner, C., Law, A. J. R., Horne, D. S., & Dalgleish, D. G. (2003). Role of the soluble and micelle-bound heat-induced protein aggregates on network formation in acid skim milk gels. *Journal of Agricultural and Food Chemistry, 51*(26), 7743–7750. https://doi.org/10.1021/jf030201x

Halabi, A., Croguennec, T., Bouhallab, S., Dupont, D., & Deglaire, A. (2020a). Modification of protein structures by altering the whey protein profile and heat treatment affects in vitro static digestion of model infant milk formulas. *Food & Function*. https://doi.org/10.1039/D0FO01362E

Halabi, A., Deglaire, A., Hamon, P., Bouhallab, S., Dupont, D., & Croguennec, T. (2020b). Kinetics of heat-induced denaturation of proteins in model infant milk formulas as a function of whey protein composition. *Food Chemistry, 302*, 125296. https://doi.org/10.1016/j.foodchem.2019.125296

Halabi, A., Deglaire, A., Hennetier, M., Violleau, F., Burel, A., Bouhallab, S., Dupont, D., & Croguennec, T. (2020c). Structural characterization of heat-induced protein aggregates in model infant milk formulas. *Food Hydrocolloids*. https://doi.org/10.1016/j.foodhyd.2020.105928, 105928.

Hodgkinson, A. J., Wallace, O. A. M., Smolenski, G., & Prosser, C. G. (2019). Gastric digestion of cow and goat milk: Peptides derived from simulated conditions of infant digestion. *Food Chemistry, 276*, 619–625. https://doi.org/10.1016/j.foodchem.2018.10.065

Huppertz, T., & Lambers, T. T. (2020). Influence of micellar calcium phosphate on in vitro gastric coagulation and digestion of milk proteins in infant formula model systems. *International Dairy Journal, 107*, 104717. https://doi.org/10.1016/j.idairyj.2020.104717

Layman, D. K., Lönnerdal, B., & Fernstrom, J. D. (2018). Applications for α-lactalbumin in human nutrition. *Nutrition Reviews, 76*(6), 444–460. https://doi.org/10.1093/nutrit/nuy004

Le Roux, L., Chacon, R., Dupont, D., Jeantet, R., Deglaire, A., & Nau, F. (2020a). In vitro static digestion reveals how plant proteins modulate model infant formula digestibility. *Food Research International, 130*. https://doi.org/10.1016/j.foodres.2019.108917

Le Roux, L., Ménard, O., Chacon, R., Dupont, D., Jeantet, R., Deglaire, A., & Nau, F. (2020b). Are Faba bean and pea proteins potential whey protein substitutes in infant formulas? An in vitro dynamic digestion approach. *Foods, 9*(3), 362. https://doi.org/10.3390/foods9030362. PubMed.

Lönnerdal, B. (2009). Nutritional roles of lactoferrin. *Current Opinion in Clinical Nutrition and Metabolic Care, 12*(3). https://journals.lww.com/co-clinicalnutrition/Fulltext/2009/05000/Nutritional_roles_of_lactoferrin.13.aspx.

Lönnerdal, B. (2016). Bioactive proteins in human milk: Health, nutrition, and implications for infant formulas. *The Journal of Pediatrics, 173*, S4–S9. https://doi.org/10.1016/j.jpeds.2016.02.070. PMID: 27234410.

Maathuis, A., Havenaar, R., He, T., & Bellmann, S. (2017). Protein digestion and quality of goat and cow milk infant formula and human milk under simulated infant conditions. *Journal of Pediatric Gastroenterology and Nutrition, 65*(6), 661–666. https://doi.org/10.1097/MPG.0000000000001740

Ménard, O., Bourlieu, C., De Oliveira, S. C., Dellarosa, N., Laghi, L., Carrière, F., Capozzi, F., Dupont, D., & Deglaire, A. (2018). A first step towards a consensus static in vitro model for simulating full-term infant digestion. *Food Chemistry, 240*, 338–345. https://doi.org/10.1016/j.foodchem.2017.07.145

Ménard, O., Cattenoz, T., Guillemin, H., Souchon, I., Deglaire, A., Dupont, D., & Picque, D. (2014). Validation of a new in vitro dynamic system to simulate infant digestion. *Food Chemistry, 145*, 1039–1045. https://doi.org/10.1016/j.foodchem.2013.09.036

Ménard, O., Picque, D., & Dupont, D. (2015). The DIDGI® system. In K. Verhoeckx, P. Cotter, I. López-Expósito, C. Kleiveland, T. Lea, A. Mackie, T. Requena, D. Swiatecka, & H. Wichers (Eds.), *The impact of food bioactives on health* (pp. 73–81). Springer International Publishing. https://doi.org/10.1007/978-3-319-16104-4_8.

Michaelsen, K. F., & Greer, F. R. (2014). Protein needs early in life and long-term health. *The American Journal of Clinical Nutrition, 99*(3), 718S–722S. https://doi.org/10.3945/ajcn.113.072603

Moughan, P. J. (1999). In vitro techniques for the assessment of the nutritive value of feed grains for pigs: A review. *Australian Journal of Agricultural Research, 50*(5), 871. https://doi.org/10.1071/AR98172

Nebbia, S., Giribaldi, M., Cavallarin, L., Bertino, E., Coscia, A., Briard-Bion, V., Ossemond, J., Henry, G., Ménard, O., Dupont, D., & Deglaire, A. (2020). Differential impact of Holder and High Temperature Short Time pasteurization on the dynamic in vitro digestion of human milk in a preterm newborn model. *Food Chemistry, 328*, 127126. https://doi.org/10.1016/j.foodchem.2020.127126

Nicoleta, S., Van der Plancken, I., Rotaru, G., & Hendrickx, M. (2008). Denaturation impact in susceptibility of beta-lactoglobulin to enzymatic hydrolysis: A kinetic study. *Revue Roumaine de Chimie, 53*.

Nielsen, S. D., Beverly, R. L., Qu, Y., & Dallas, D. C. (2017). Milk bioactive peptide database: A comprehensive database of milk protein-derived bioactive peptides and novel visualization. *Food Chemistry, 232*, 673–682. https://doi.org/10.1016/j.foodchem.2017.04.056

de Oliveira, S. C., Deglaire, A., Ménard, O., Bellanger, A., Rousseau, F., Henry, G., Dirson, E., Carrière, F., Dupont, D., & Bourlieu, C. (2016). Holder pasteurization impacts the proteolysis, lipolysis and disintegration of human milk under in vitro dynamic term newborn digestion. *Food Research International, 88*, 263–275. https://doi.org/10.1016/j.foodres.2015.11.022

Picariello, G., Ferranti, P., Fierro, O., Mamone, G., Caira, S., Di Luccia, A., Monica, S., & Addeo, F. (2010). Peptides surviving the simulated gastrointestinal digestion of milk proteins: Biological and toxicological implications. *Journal of Chromatography B, 878*(3), 295–308. https://doi.org/10.1016/j.jchromb.2009.11.033

Picariello, G., Miralles, B., Mamone, G., Sanchez-Rivera, L., Recio, I., Addeo, F., & Ferranti, P. (2015). Role of intestinal brush border peptidases in the simulated digestion of milk proteins. *Molecular Nutrition & Food Research, 59*. https://doi.org/10.1002/mnfr.201400856

Rastogi, N., Singh, A., Pandey, S. N., Sinha, M., Bhushan, A., Kaur, P., Sharma, S., & Singh, T. P. (2014). Structure of the iron-free true C-terminal half of bovine lactoferrin produced by tryptic digestion and its functional significance in the gut. *FEBS Journal, 281*(12), 2871–2882. https://doi.org/10.1111/febs.12827

Sánchez-Rivera, L., Ménard, O., Recio, I., & Dupont, D. (2015). Peptide mapping during dynamic gastric digestion of heated and unheated skimmed milk powder. *FOOD BIOACTIVE COMPOUNDS: QUALITY CONTROL AND BIOACTIVITY, 77*, 132–139. https://doi.org/10.1016/j.foodres.2015.08.001

Sanchón, J., Fernández-Tomé, S., Miralles, B., Hernández-Ledesma, B., Tomé, D., Gaudichon, C., & Recio, I. (2018). Protein degradation and peptide release from milk proteins in human jejunum. Comparison with in vitro gastrointestinal simulation. *Food Chemistry, 239*, 486–494. https://doi.org/10.1016/j.foodchem.2017.06.134

Sandström, O., Lönnerdal, B., Graverholt, G., & Hernell, O. (2008). Effects of α-lactalbumin–enriched formula containing different concentrations of glycomacropeptide on infant nutrition. *The American Journal of Clinical Nutrition, 87*(4), 921–928. https://doi.org/10.1093/ajcn/87.4.921

Sharma, S., Sinha, M., Kaushik, S., Kaur, P., & Singh, T. P. (2013). C-lobe of lactoferrin: The whole story of the half-molecule. *Biochemistry Research International*, 1–8. https://doi.org/10.1155/2013/271641, 2013.

Sreedhara, A., Flengsrud, R., Langsrud, T., Kaul, P., Prakash, V., & Vegarud, G. E. (2010). Structural characteristic, pH and thermal stabilities of apo and holo forms of caprine and bovine lactoferrins. *Biometals, 23*(6), 1159–1170. https://doi.org/10.1007/s10534-010-9366-5

Stănciuc, N., Aprodu, I., Râpeanu, G., van der Plancken, I., Bahrim, G., & Hendrickx, M. (2013). Analysis of the thermally induced structural changes of bovine lactoferrin. *Journal of Agricultural and Food Chemistry, 61*(9), 2234–2243. https://doi.org/10.1021/jf305178s

Tam, J. J., & Whitaker, J. R. (1972). Rates and extents of hydrolysis of several caseins by pepsin, rennin, endothia parasitica protease and mucor pusillus protease. *Journal of Dairy Science, 55*(11), 1523–1531. https://doi.org/10.3168/jds.S0022-0302(72)85714-X

Totzauer, M., Luque, V., Escribano, J., Closa-Monasterolo, R., Verduci, E., ReDionigi, A., Hoyos, J., Langhendries, J.-P., Gruszfeld, D., Socha, P., Koletzko, B., & Grote, V., for The European Childhood Obesity Trial Study Group. (2018). Effect of lower versus higher protein content in infant formula through the first year on body composition from 1 to 6 Years: Follow-up of a randomized clinical trial. *Obesity, 26*(7), 1203–1210. https://doi.org/10.1002/oby.22203

Trabulsi, J., Capeding, R., Lebumfacil, J., Ramanujam, K., Feng, P., McSweeney, S., Harris, B., & DeRusso, P. (2011). Effect of an α-lactalbumin-enriched infant formula with lower protein on growth. *European Journal of Clinical Nutrition, 65*(2), 167–174. https://doi.org/10.1038/ejcn.2010.236

Wada, Y., Phinney, B. S., Weber, D., & Lönnerdal, B. (2017). In vivo digestomics of milk proteins in human milk and infant formula using a suckling rat pup model. *Peptides, 88*, 18–31. https://doi.org/10.1016/j.peptides.2016.11.012

Wang, B., Timilsena, Y. P., Blanch, E., Adhikari, B., & Lactoferrin. (2019). Structure, function, denaturation and digestion. *Critical Reviews in Food Science and Nutrition, 59*(4), 580–596. https://doi.org/10.1080/10408398.2017.1381583

Ye, A., Cui, J., Dalgleish, D., & Singh, H. (2016). Formation of a structured clot during the gastric digestion of milk: Impact on the rate of protein hydrolysis. *Food Hydrocolloids, 52*, 478–486. https://doi.org/10.1016/j.foodhyd.2015.07.023

Zenker, H. E., Wichers, H. J., Tomassen, M. M. M., Boeren, S., De Jong, N. W., & Hettinga, K. A. (2020). Peptide release after simulated infant in vitro digestion of dry heated cow's milk protein and transport of potentially immunoreactive peptides across the caco-2 cell monolayer. *Nutrients, 12*(8), 2483. https://doi.org/10.3390/nu12082483